CLM - P 321

UKAEA RESEARCH GROUP

Preprint

STARK BROADENING OF HIGH QUANTUM NUMBER $\Delta n=1$ TRANSITIONS OF CARBON V AND VI IN A LASER-PRODUCED PLASMA

F E IRONS

CULHAM LABORATORY
Abingdon Berkshire

1972

CLM-P 321

STARK BROADENING OF HIGH QUANTUM NUMBER $\Delta n=1$ TRANSITIONS OF CARBON V AND VI IN A LASER-PRODUCED PLASMA

F E Irons*

(To be submitted for publication in Journal of Physics B, Atomic and Molecular Physics)

ABSTRACT

Stark-broadened wavelength profiles of the hydrogen-like lines carbon VI (6-7) 3434, (7-8) 5290 Å and the quasi hydrogen-like lines carbon V (5-6) 2982, (6-7) 4945 Å have been recorded, with time resolution, in the high density plasma produced by the laser-irradiation of a polyethylene foil in vacuum. Stark theory of relevance to these new lines is reviewed. Half-widths are calculated for values of electron and ion density deduced from line intensities, and are compared with experiment. It is shown that the broadening is predominantly ion quasi-static, with C^{6+} and C^{5+} as the principal perturbing ions. The electron impact contribution to the broadening would be at least as great as the ion contribution if it were not for correlations in the perturbations of the upper and lower states. There is a factor of two difference between theory and experiment, which is about the maximum which can be explained in terms of errors in the experiment and in the formulation of the Stark theory.

* Now at The Department of Engineering Physics, Research School of Physical Sciences, Australian National University, Box 4 P.O. Canberra, A.C.T. 2600, Australia.

U.K.A.E.A. Research Group,
Culham Laboratory,
Abingdon,
Berks.

June, 1972

1. INTRODUCTION

Recently, new spectral lines of carbon V and VI have been observed in the plasma produced when a Q switched ruby laser pulse is focussed onto a polyethylene foil in vacuum (Boland et al 1968, hereafter called Paper I). Amongst the strongest of these new lines are transitions of the type $\Delta n = 1$ (where n denotes principal quantum number), some of which originate from high n states and fall in the spectral range $\lambda\lambda$ 2100-6000 Å. These are listed below in Table 1. The appearance of such lines can be related to the high density ($> 10^{17} cm^{-3}$) of highly stripped ions which is characteristic of laser-produced plasmas.

Table 1

Line	Transition
C VI 5290	7 - 8
C VI 3434	6 - 7
C V 4945	6 - 7
C V 2982	5 - 6

Some of the lines in Table 1 have been observed in beam-foil interactions (e.g. Bashkin, 1970), and in the plasma focus source (by the author, unpublished), and in a theta-pinch plasma (a tentative identification by Pasco and Smeulders of this laboratory, unpublished). A similar line of lithium III has been reported in a laser-produced plasma (Ambartsumyan et al., 1965).

The lines in Table 1, being hydrogen-like (C VI) and quasi hydrogen-like (C V), show strong first order Stark broadening, which is the subject of study in this paper. The laser-produced plasma studied here (the same as in paper I) is formed at the target surface, with

an electron temperature of $T_e \gtrsim 100$ eV, and expands rapidly into the vacuum environment, preferentially along the target normal (the dynamics of the plasma expansion has been studied in a separate paper, Irons et al, 1972, hereafter called paper II). Observations are made at distances ≥ 1 mm from the target, where $T_e \leq 34$ eV and the electron density, $N_e \leq 3 \times 10^{18} cm^{-3}$. At each point of observation the CV and C VI emission is observed for a period of ~ 40 nanoseconds as the plasma expands past the point of observation.

The method of analysis adopted here has been to deduce electron and ion densities from line intensities and to predict line widths using a theory (suggested to the author by Griem) based on an extension of currently available theory. The predicted line widths are then compared with experiment. Uncertainties in the predictions amount to about $\pm$ 50%, which is about the measure of agreement with experiment. Of greater precision however is the theoretical prediction of the scaling of line widths with parameters such as principal quantum number, nuclear charge and density, and here a comparison between theory and experiment identifies which particle species (ions or electrons) is mainly responsbile for the broadening and which theory (quasi-static or impact) is the more relevant.

Previous studies of Stark broadening in laser-produced plasmas have included the Balmer lines of H and He II and several isolated lines of neutral and singly ionised atoms, and the broadening has either been used to give a measurement of density (Litvak and Edwards, 1966; Bacon, 1969) or has been shown to be in fair agreement with theory (Ramsden and Davies, 1964; Mandel'shtam et al., 1964; Evtushenko et al., 1966). Estimates of density from the Stark

broadening of multiply-ionised species in laser-produced plasmas have been reported for O VI, K IX (Burgess et al.,1967) and for C VI (discussed later in section 2.4). An earlier report of visible quasi hydrogen-like lines (of nitrogen V, in a toroidal Z pinch) with a comment on their Stark broadening and their usefulness for measuring density, can be found in the paper of Hallin and Hughes (1961).

2. STARK THEORY FOR HIGHER HYDROGEN-LIKE $\Delta n = 1$ TRANSITIONS

In this section Stark theory of relevance to the lines in Table 1 is reviewed, and expressions are proposed for the half-widths in the ion quasi-static, electron impact and ion impact theories. The ion impact theory is included because substitution into the relevant criterion (section 6.2.2) shows that it is of marginal interest: the electron quasi-static broadening is excluded because a similar substitution shows that it is of no interest.

2.1. Ion Quasi-Static Theory

An expression for the half-width in the ion quasi-static theory may be derived by considering averages (Griem- private communication). The (angular frequency) displacement of a typical first order Stark component of a hydrogen-like line in an electric field F is given by

$$\Delta\omega = \frac{3}{2}\,\frac{\hbar}{meZ}\left[\, n_u\,(n_1 - n_2)_u - n_\ell (n_1 - n_2)_\ell \,\right] F \qquad (1)$$

where Z is the nuclear charge, n is the principal quantum number, n_1 and n_2 are parabolic quantum numbers, and the subscripts u and ℓ denote the upper and lower states respectively. This formula is valid for lines of the hydrogen-like ion C VI ($Z = 6$) and also for transitions amongst the high quantum states of C V ($Z = 5$) which are largely degenerate (the degeneracy of C V is discussed in section 4.2).

A first approximation to the full half-width is obtained by averaging equation (1) and doubling, viz.

$$\Delta\omega_{\frac{1}{2}} = 2\,\overline{\Delta\omega} = 2 \times \frac{3}{2}\frac{\hbar}{meZ}\,(n_\ell + \tfrac{1}{2}) \times 8.8\, e\, Z_p\, N_p^{2/3} \qquad (2)$$

where we have put

$$\overline{\left[n_u(n_1 - n_2)_u - n_\ell\,(n_1 - n_2)_\ell \right]} \approx \tfrac{1}{2}\,(n^2_u - n^2_\ell)$$

$$\approx n_\ell + \tfrac{1}{2} \text{ (when } n_u - n_\ell = 1)$$

and where, for one species of perturbing ion, of charge Z_p and density N_p

$$\overline{F} = 8.8\, e\, Z_p\, N_p^{2/3} \text{ (Holtsmark approximation)}$$

$$= 8.8\, e\, Z_p^{1/3} N_e^{2/3} \text{ (putting } N_e = Z_p N_p). \qquad (3)$$

For more than one species of perturbing ion the expression for $\overline{F}$ must allow for the vectorial addition of the various ion fields, and is given approximately by equation (3) with a suitable mean value for Z_p, with N_e now denoting the total electron density. The choice of a mean value for Z_p introduces only a small error into equation (3) because Z_p is raised to the one-third power.

Some justification of the averaging process which led to equation (2) can be found in the paper of Griem (1960), where it is shown that, in the Holtsmark approximation, the Stark profiles of the higher members of the Balmer and other series of hydrogen scale according to an 'average profile', the half-width of which is equal to that given by equation (2) to within 15%.

The expression for $\overline{F}$ (equation (3)) is based on the Holtsmark approximation and is valid only at low densities where electron (Debye) screening and ion-ion interactions are negligible, i.e. where

$$\frac{e^2 N_e}{kT_e N_p^{1/3}} < 0.1 \text{ (Debye screening)}$$

and

$$\frac{Z_p^2 e^2 N_p^{1/3} \pi}{M \langle v \rangle^2} < 0.1 \text{ (ion-ion interactions)}$$

where M is the ion mass and $\langle v \rangle$ is the mean ion relative velocity (discussed in section 2.3). A third inequality should be included for emitter-perturber interactions, but this is essentially the same as the second inequality above, which is for perturber-perturber interactions. The above expressions, when evaluated with the plasma parameters in sections 2.3 and 4.3 give values of ~ 0.4 (Debye screening) and ~ 0.1 (ion-ion interactions). The effects concerned cannot therefore be neglected: in fact a calculation based on Hooper (1967) and Margenau and Lewis (1958) shows that the ion microfield will be reduced by a factor of about two. It is assumed that the half-width is reduced by a similar factor; giving as a final expression for the full half-width, with an error of about $\pm$ 30%

$$\Delta\omega_{\frac{1}{2}} = 2 \times \frac{3}{2} \frac{\hbar}{meZ} (n_\ell + \tfrac{1}{2}) \times \tfrac{1}{2} \times 8.8\, e\, Z_p^{1/3} N_e^{2/3} \quad . \qquad (4)$$

2.2. Electron Impact Theory

An expression for the electron (elastic) impact half-width of a line from a hydrogen-like ion can be found in an early paper of Griem (1960); though as pointed out later (Griem, 1967 a,b) this expression

is strictly valid only for low series members (and needs to be multiplied by $\sim \frac{6.75}{n}$ for high series members), and also needs to be corrected for correlations in the perturbations of the upper and lower states, which are especially important for higher transitions of the type $\Delta n = 1$.

A theory of impact broadening has been developed by Griem (1967 b) for the n_α lines of hydrogen (i.e. lines with $\Delta n = 1$ where $n \gtrsim 150$: these are observed in the radio spectrum of certain nebulae - for a recent review see Dupree and Goldberg, 1970). A similar theory is applicable to the present lines, and the full half-width, including both inelastic collisions (from the Born approximation) and elastic collisions, may be expressed as (Griem, private communication)

$$\Delta\omega_{\frac{1}{2}} = \frac{8\pi^2}{3^{3/2}} \left(\frac{2m}{\pi kT_e}\right)^{\frac{1}{2}} \left(\frac{\hbar n_\ell}{mZ}\right)^2 \left(\frac{n_\ell^2}{2} + \frac{9}{2}\right) \bar{g} N_e \qquad (5)$$

($\frac{n_\ell^2}{2}$: inelastic; $\frac{9}{2}$: elastic (with correlations))

where

$$\bar{g} = \frac{3^{\frac{1}{2}}}{\pi} \left[\tfrac{1}{2} + \ln\left(\frac{3n_\ell\, kT_e}{8\, Z\, I_H}\right)\right] .$$

The gaunt factor, $\bar{g}$, is of order unity at the times of interest in the present plasma. The various approximations in deriving equation (5) are valid to within 30% for $n_\ell > 6$. At lower n_ℓ some improvement is to use $n_\ell + \frac{1}{2}$ instead of n_ℓ, as has been done here. Equation (5) is unlikely to be in error by more than a factor of two.

The effect of correlated perturbations between the upper and lower states is to reduce the elastic impact half-width by about

$\times \frac{1}{n_\ell^2}$ ($\times \frac{1}{40}$ in the present case), and the total half-width (elastic + inelastic) by about $\times \frac{1}{8}$.

2.3. Ion Impact Theory

Also in connection with the n_α lines of hydrogen, Griem has derived an expression for the half half-width in the ion impact approximation (Griem, 1967 b). This expression, when scaled for the charge of the perturbing ions, Z_p, becomes (Griem, private communication)

$$\Delta\omega_{ci} = \frac{3\pi}{\langle v\rangle}\left(\frac{\hbar}{m}\right)^2 n_\ell^{\,2}\left[\tfrac{1}{2} + \frac{2}{e^2}\ln\frac{2\,n_\ell}{3}\right]\left\{\tfrac{1}{2} + \ln\left(\frac{m\lambda\langle v\rangle}{2\pi^{3/2}\hbar\, n_\ell}\right)\right\} Z_p^2\, N_p \qquad (6)$$

where N_p is the number density of perturbing ions, and $\langle v\rangle$ is the mean ion relative velocity, i.e. the mean velocity in the frame of reference of the expanding plasma. Note that this relative velocity distribution may not be thermal since the plasma expansion takes place on a time scale comparable with the ion-ion collision time. For the region a few millimetres from the target a value of $\langle v\rangle \approx 3 \times 10^6 \text{cm s}^{-1}$ has been estimated from Doppler broadening (as distinct form shifting - see paper II), and from the increasing time spread of C V and C VI line radiation with distance from the target (paper I). Interestingly enough this value of $\langle v\rangle$ is approximately equal to a mean thermal velocity for the same region, with the ion temperature equal to the measured electron temperature.

Equation (6) contains only the elastic term (modified for correlated perturbations) because the inelastic term is negligible by comparison. Equation (6) may be scaled to give the half-width of a

$\Delta n = 1$ transition from a hydrogen-like ion of nuclear charge Z viz.

$$\Delta\omega_{\frac{1}{2}} = \frac{2\Delta\omega_{ci}}{Z^2} \qquad (7)$$

where $\Delta\omega_{\frac{1}{2}}$ now denotes full half-width.

2.4. Comments on Other Studies of C VI

Earlier studies of C VI (Boland and Irons 1967; Aglitzky et al., 1970), both with laser-produced plasmas, have used the theory of Griem (1960) with suitable Z_p scaling to interpret the broadening to give density. This theory is for hydrogen-like transitions where $\Delta n \sim n$. The adoption of this theory (with Z_p scaling) gives a fair representation of the ion quasi-static broadening, but grossly over-estimates the electron impact contribution for transitions $\Delta n = 1$ at high n, and would have led the above authors to underestimate the density by a factor of between two and three (for C VI 3434 Å).

Aglitzky et al. (1970) have considered the Stark theory in some detail, and have applied it to the lines C VI (6-7) 3434 and C VI (3-4) 521 Å. The latter line enables them to estimate density as close as 0.1 mm to the target (at this wavelength there is not the strong continuum which prohibits line profile measurements closer than 1 mm to the target in the visible and near u.v. region of the spectrum). They emphasize the value of such a measurement in giving the density during the formative period of the plasma.

A comparison will also be made between the present experimental results and the theoretical calculations of Peach (e.g. Peach 1971).

3. EXPERIMENTAL ARRANGEMENT

Reference should be made to paper I for full details of the experimental arrangement. Briefly the plasma is formed when the Q switched pulse from a Korad K 1500 ruby laser system, of energy 5 J and duration 17 ns at half maximum intensity, is focused by a 10 cm focal length lens into a vacuum chamber, so as to fall at normal incidence onto a polyethylene $(C_2H_4)_n$ foil, 0.25 mm thick, with an average light flux of 2.9×10^{11} W cm^{-2}.

The laser axis, or target normal at the focal point is defined as the x axis, with the focal point as the origin. Time is measured from the time of arrival of the leading edge of the laser pulse at the target, and on this scale the time to peak laser intensity corresponds to $t = 20$ ns.

Light from the plasma, emitted at right angles to the x axis, was focused by a quartz-lithium fluoride achromat onto the entrance slit of a 1.5 m focal length Ebert monochromator, the signal at the exit slit being monitored by a photomultiplier (EMI 9594 QB) and then displayed on a Tektronix 519 oscillopscope and photographed. The instrumental rise-time was measured to be $\sim$ 3 ns. The complete optical system was calibrated in situ for absolute intensities by means of a tungsten strip lamp. This calibration was extended below the lower wavelength limit of the lamp (3300 Å) to the lowest wavelength of interest (2982 Å) by means of the plasma continuum (with a wavelength dependence λ^{-3} as measured at wavelengths $>$ 3300 Å).

4. LINE INTENSITIES: DETERMINATION OF DENSITY

In paper I it was shown that the upper quantum states of an ion in a laser-produced plasma were in near L.T.E. (Local Thermal Equilibrium) with the next ion stage, and that the intensity of a line from such a state, of an ion of charge Z-1, could be related to the density of the next ion stage $N(C^{z+})$ and the electron density N_e by means of the Saha-Boltzmann equation, multiplied by a factor r to allow for small departures from L.T.E., viz,

$$I = r\left(\frac{h^2}{2\pi mkT_e}\right)^{\frac{3}{2}} \frac{\omega A h\nu}{2\omega(C^{z+})\ 4\pi} N_e\ N(C^{z+})\ \exp\left(\frac{\chi}{kT_e}\right) \times \text{plasma depth} \qquad (8)$$

where the symbols are as defined in paper I, and values of r for hydrogen-like ions are listed in McWhirter and Hearn (1963).

The equation of charge neutrality provides an additional relationship between electron and ion densities, in the present case of the form

$$N_e = f\left\{N(C^{6+}),\ N(C^{5+})\right\} . \qquad (9)$$

The simultaneous solution of equations 8 and 9 gives the densities N_e, $N(C^{5+})$ and $N(C^{6+})$.

The densities derived in paper I suffered from an uncertainty in the 'plasma depth' which appears in equation 8 and in the form of equation 9. New measurements of spatial distribution remove these uncertainties (section 4.1), and when combined with more accurate values of C V transition probabilities (section 4.2) and more accurate measurements of the line intensities, give improved values of density (section 4.3). A comment is included on the departure from L.T.E.

4.1. Ion Spatial Distribution

The line emission C VI (5-6) 2070 Å and C V ($2s^3S$-$2p^3P$) 2271 Å was scanned at right angles to the x axis to give the 'radial' spatial distribution of the regions of C VI and C V emission, using the technique described in paper II. Smooth curves of best fit to the data points are shown in figure 1, for the two distances x = 1.0 and 1.6 mm.

An inspection of figure 1 shows that the time development of the spatial distribution may, to a good approximation, be considered in three periods, viz a period early in time ($t \leq 30$ ns) when the C VI and C V emissions are spatially separate; an intermediate period of gradual merging; and a period later in time ($t \geq 40$ ns) when the C VI and C V emissions are spatially coincident. Attention is fixed on the first and third periods, hereafter called the periods of 'separate emission' and 'coincident emission' respectively, since in these periods equation 9 takes on a simple form, as indicated in Table 2.

TABLE 2

Period	Charge neutrality (including H^+ ions)
Separate emission	$N_e = 8\ N(C^{6+})$ for C VI $N_e = 7\ N(C^{5+})$ for C V
Coincident emission	$N_e = 8\ N(C^{6+}) + 7\ N(C^{5+})$

The H^+ ions have been included in these equations because the observations of Faugeras et al. (1968) and Mattioli and Veron (1969, 1970) indicate that H^+ ions are present in the fastest parts of the plasma from hydrogenous targets. The value assumed for the ratio $N(H^+) : N(C^{z+})$ (= 2:1, as in the target material) is not critical as regards the values calculated for N_e and $N(C^{z+})$, partly because most of the electrons come from the ions C^{z+}, and partly because of the restriction imposed on the product $N_e N(C^{z+})$ by equation 8.

Note that $N(C^{4+})$ is not included in Table 2 because the C IV emission merges with C V later than when C VI is still present (as inferred from the results in paper II).

4.2. CV Transition Probabilities

Calculations based on the recent C V term scheme of Edlén and Löfstrand (1970) indicate that transitions amongst substates $L \geq D$ contribute to the C V line intensities. This gives values for the transition probabilities (calculated by the method of Bates and Damgaard, 1949) of $\omega A = 5.2 \times 10^{10} s^{-1}$ (C V 4945) and $= 8.3 \times 10^{10} s^{-1}$ (C V 2982), which are a slight improvement over those in paper I (which had included transition amongst substates $L \geq F$).

The criterion adopted above for a transition to contribute to the line intensity is that it should fall within two (observed) half-widths of the line centre. The observed half-width is however a reduced estimate of the quantum state perturbation (i.e. reduced by correlations, see section 2.2). A calculation, using as a criterion not the observed half-widths but the quantum state perturbation (estimated from Griem, 1960), indicates that the transitions D - P and P - D may also contribute. These additional transitions are,

however, of negligible intensity.

The transition probabilities for C VI were calculated by scaling those for hydrogen (from Wiese et al, 1966) by $Z^4 = 6^4$.

4.3. Determination of Density

To measure a line intensity with the greatest signal-to-noise (i.e. line-to-continuum) ratio, a measurement was made of the intensity of a small wavelength band (8.1 Å) at the line CENTRE (the mean of six shots) and was multiplied by the appropriate ratio (determined from the line profiles) to give the total line intensity; with a correction being made for the continuum. With this procedure all the intensities could be measured on the one run, with an absolute intensity calibration at the beginning and end of the run.

When measuring density we distinguish between the regions $x \leq 2$ mm and $x > 2$ mm. In the region $x \leq 2$ mm we have values of T_e deduced independently from spectrum photographs of the free-bound continuum (paper I). These values (equal to 34 eV at x = 1.0 mm and 16 eV at x = 1.6 mm) are approximately the same for C V and VI, indicating that there is no significant variation of T_e over the times of interest here. The simultaneous solution of equations 8 and 9 for C VI 5290 and for C V 4945, using the above values of T_e and values of 'plasma depth' from figure 1, gives the values of density shown in Table 3.

TABLE 3

Electron and Ion Densities

x	Period	N_e cm^{-3}	$N(C^{6+})$ cm^{-3}	$N(C^{5+})$ cm^{-3}	$N(H^+)$ cm^{-3}
1.0 mm	Separate	2.1×10^{18}	2.2×10^{17}	3.4×10^{17}	$\sim 6 \times 10^{17}$
1.0 mm	Coincident	3.2×10^{18}	0.7×10^{17}	3.6×10^{17}	$\sim 9 \times 10^{17}$
1.6 mm	Separate	0.7×10^{18}	0.8×10^{17}	1.0×10^{17}	$\sim 2 \times 10^{17}$
1.6 mm	Coincident	0.7×10^{18}	0.3×10^{17}	0.7×10^{17}	$\sim 2 \times 10^{17}$

At the distances x = 1.0 and 1.6 mm of the above measurements, the theory of McWhirter and Hearn (1963) indicates that the factor r in equation 8 should be within a few percent of unity for each of the lines C VI 3434, 5290 Å and C V 2982, 4945 Å. Also the ratio of intensities $\frac{I(5290)}{I(3434)}$ and $\frac{I(4945)}{I(2982)}$ should be independent of density and only slightly dependent on temperature. A comparison of the theoretical and experimental values of these ratios (fig. 3) shows that there is fair agreement for C VI, but that the experimental values of C V are significantly smaller than the theoretical values. The C V intensities were remeasured, with the same result, which remains unexplained.

In the region x > 2 mm the free-bound continuum could not be detected and we do not have an independent measurement of T_e. However in this region the temperature has fallen sufficiently for the temperature dependent part of equation 8 to be significantly different for the two lines of each ion. The simultaneous solution

of equations 8 and 9, firstly for the two lines of C VI and secondly for the two lines of C V now gives values of density (fig. 2) and of temperature. The values of T_e are 8 $\pm$ 3 eV (C VI) and 9 $\pm$ 3 eV (C V) at x = 2.8 mm, and 3.5 $\pm$ 1 eV (C VI) and 5 $\pm$ 2 eV (C V) at x = 5.0 mm.

Figure 2 shows the values of N_e deduced from line intensities. In another experiment (Aglitzky et al, 1971) values of N_e have been deduced from interferometry on a plasma similar to that studied here i.e. a plasma produced from a carbon target with a neodymium laser of energy $\sim$ 10 J and pulse duration $\sim$ 15 ns. The values of N_e deduced by these authors at a time 36 ns after the beginning of the laser pulse (which is about the time of interest here) are also shown in fig. 2. There is good agreement between the two sets of measurements, at least in the limited region where they overlap. Other (interferometric) measurements of density, under experimental conditions which are only partly compatible with those used here (Basov et al, 1968), give values of density which are within a factor of two of those measured here.

5. LINE PROFILES: RESULTS

Line (wavelength) profiles were built up on a shot-to-shot basis with typically two or three shots being recorded at each of some fifty points across the profile. Shots were rejected if the peak laser intensity, as monitored with a photodiode, varied more that $\pm$ 20% from the mean. The data was collated at 5 ns intervals over the 40 ns duration of each light pulse.

To study the relative contribution of Stark and Doppler effects, line profiles were recorded at a number of distances in the range x = 1 - 12 mm, the direction of sight passing through the x axis at

right angles. At distances x < 1 mm the profiles were difficult to measure above the continuum. Stark profiles typical of those recorded close to the target, at x = 1.0 and 1.6 mm, are shown in figures 4 - 7 (profiles are shown for two distances, corresponding to two different values of density, to assist with the future fitting of theoretical profiles). Doppler profiles recorded far from the target at x = 12 mm, are shown in figure 8. Doppler profiles were also recorded for the line C V 2271 Å which has negligible Stark effect and shows only Doppler broadening at any distance (figures 8 and 9; and note that the width of these profiles about the peaks is limited by the instrumental profile of full half-width 0.30 Å). The Doppler profiles vary in time (paper II), and those shown in figures 8 and 9 are for the period of separate emission.

In figures 4 - 9 the data for the two or three shots at each wavelength have been joined by vertical lines to give an indication of the shot-to-shot spread in intensity, and in some cases a smooth curve has been drawn to give a visual best fit. The Stark profiles are shown into the wings to the point where the experimental error is comparable to the intensity of the line above the continuum- the continuum being determined from data points up to 300 Å either side of the line centre. Most profiles are fairly symmetrical, though C VI 3434 tends to be slightly asymmetrical at around the time of peak intensity.

5.1. Half-widths

Time average values of the half-widths have been plotted in figure 10 as a function of distance from the target, and have been joined by smooth curves to show the trend, viz the broadening decreases

rapidly with distance to x $\underset{\sim}{>}$ 5 mm beyond which there is no significant decrease.

At x = 1.0 and 1.6 mm the C VI half-widths vary in time by $\pm$ 10%. Likewise for C V at x = 1.0 mm; though at x = 1.6 mm the C V half-widths vary as 16 - 23 - 9 Å (C V 4945) and 6.5 - 7.5 - 5.0 Å (C V 2982) from the start-to the peak-to the end of the C V light pulse respectively. At x = 2.8 and 5.0 mm the half-width of the two C V lines decrease in time by $\sim$ 40% over the period of each light pulse.

There is good agreement between the half-widths of C VI 3434 at x = 1.0 mm reported here and those reported by Aglitzky et al, (1970) from photographs of the spectrum of a similar (neodymium) laser-produced plasma from a carbon target.

Values of the half-width ratio $\frac{\Delta\lambda_{\frac{1}{2}}\ 5290}{\Delta\lambda_{\frac{1}{2}}\ 3434}$ for C VI and $\frac{\Delta\lambda_{\frac{1}{2}}\ 4945}{\Delta\lambda_{\frac{1}{2}}\ 2982}$ for C V were calculated form the observed half-widths $\Delta\lambda_{\frac{1}{2}}$, and time-averages values are shown in figure 11. Both ratios were found to be constant in time to within 10% of the mean at x = 1.0 mm and 1.6 mm; whereas they both decreased in time by up to 60% at x = 2.8 and 5.0 mm.

6. LINE PROFILES: INTERPRETATION

6.1. Separation of Doppler and Stark Effects

Doppler broadening, produced by the streaming motion of the ions, is present in all lines and was the subject of study in paper II. As a result of that study the two-peaked profiles observed with C V (figures 8 and 9) are recognised as Doppler in origin; with the peaks displaced to the low and high wavelength side of the normal line centre representing motion of sections of the plasma towards and away from the observer respectively. Such profiles are observed with all C V

lines at x = 12 mm (figure 8) and indicate the purely Doppler nature of the broadening at this distance.

Figure 11 shows experimental values of the half-width ratios $\frac{\Delta\lambda_{\frac{1}{2}}5290}{\Delta\lambda_{\frac{1}{2}}3434}$ and $\frac{\Delta\lambda_{\frac{1}{2}}4945}{\Delta\lambda_{\frac{1}{2}}2982}$. Also shown, on the right-hand ordinate are theoretical values of the same ratios for Doppler broadening (the ratio of wavelengths) and for Stark broadening (from equations 4, 5 and 7). At x = 12 mm the experimental half-widths are in agreement with the Doppler values, and only at distances x < 5 mm do the experimental values deviate from Doppler and approach Stark values.

The Doppler contribution to the lines C V 4945 and C V 2982 at distances x < 5 mm can be calculated in two ways, with the same result, viz, either by wavelength scaling the (observed) Doppler broadening of C V 2271, or by noting that the Doppler broadening of C V 2271 (and hence of the other C V lines) is constant over the range 0.35 - 12 mm, and in particular is equal to that observed at x = 12 mm. The broadening observed with C V 4945 and C V 2982 close to the target is much greater than the Doppler contribution and must therefore be due to the Stark effect.

The Doppler contribution to the lines C VI 5290 and C VI 3434 at distances x < 5 mm can be estimated from the velocity measurements in paper II. Alternatively an upper limit to the Doppler contribution to these lines can be calculated by wavelength scaling the observed broadening of C VI 2070 Å also shown in figure 10 (at x = 1.0 and 1.6 mm this line has comparable Stark and Doppler components). Either way it is found that the majority of the broadening close to the target is due to the Stark effect.

6.2. Stark Broadening; Comparison with Theory

A comparison with theory is made of various half-width ratios (section 6.2.1) and of absolute half-widths (section 6.2.2).

The observed line profiles have beeen compared with early results of the theory of Peach (1971, and private communication). A good match was achieved with theoretical profiles whose densities were about half those measured from line intensities (Table 2). A more complete comparison must await future theoretical developments.

It is of interest to note that a curve of the form $I \sim (\Delta\lambda)^{-\alpha}$ where $\Delta\lambda$ denotes wavelength displacement from the line centre, was fitted to all of the Stark profiles at x = 1.0 and 1.6 mm, and that, with each line, the curve of best fit corresponded to $\alpha = 1.5 \pm 0.4$ for the region of the profile from the half-width to twice the half-width, and to $\alpha = 2.3 \pm 0.4$ for the region beyond twice the half-width. A value of $\alpha = 2.5$ is expected for ion quasi-static broadening; $\alpha < 2.5$ for impact broadening; and $\alpha > 2.5$ for broadening in the electric field of waves (e.g. Griem and Kunze, 1969). However the number 2.5 will need to be modified for the effects of electron shielding and ion-ion correlations.

Note that the criterion of Cooper (1966) for the optical transparency of a dispersive line profile was satisfied by all the lines considered here.

6.2.1. Relative Half-widths

The ion quasi-static, electron impact and ion impact half-widths (equations 4, 5, and 7 respectively) are all functions of principal quantum number, of nuclear charge and of plasma parameters (mainly density). By a suitable choice of lines it is possible to isolate each

of these functional dependences and to obtain three separate comparisons between experiment and theory.

(i) The dependence on principal quantum number is got from lines of the same ion, i.e. from the half-width ratios $\frac{\Delta\lambda_{\frac{1}{2}}5290}{\Delta\lambda_{\frac{1}{2}}3434}$ for C VI and $\frac{\Delta\lambda_{\frac{1}{2}}4945}{\Delta\lambda_{\frac{1}{2}}2982}$ for C V, in figure 11. Theoretical values are marked on the right-hand ordinate in this figure. For the electron and ion impact values there is an additional weak dependence on T_e and $\langle v \rangle$ respectively. For the ion impact theory, a mean value and lower limit have been calculated, using respectively, $\langle v \rangle = 3 \times 10^6$ cm s^{-1} (the probable value, see section 2.3) and 3×10^7 cm s^{-1} (the expansion velocity, and well above the likely maximum). Comparing theory and experiment close to the target where Stark broadening is dominant, we find good agreement with the ion quasi-static theory for both C VI and C V, and poor agreement, well outside the experimental limits for the electron and ion impact theories.

(ii) The dependence on nuclear charge is got from lines with the same principal quantum numbers but coming from different ions, viz, C VI (6-7)3434 and C V (6-7)4945. We fix our attention on the period of coincident emission since here the perturbing forces on both lines are the same. The half-width ratio $\frac{\Delta\lambda_{\frac{1}{2}}3434}{\Delta\lambda_{\frac{1}{2}}4945}$ is approximately the same at x = 1.0 and 1.6 mm and has an average value of 0.35 $\pm$ .08. This is in fair agreement with the ion quasi-static value (0.40) and with the electron impact value (0.32 $\pm$ .03) but in poor agreement with the ion impact value (0.23 $\pm$ .05).

(iii) The dependence on plasma parameters (mainly density) is got for each line from the variation of the half-width with distance from the target. The ratio of half-widths between x = 1.0 and 1.6 mm was

found to be approximately the same for all lines and has an average value of 0.56 $\pm$ .06. This is in good agreement with the ion quasi-static value (0.50 $\pm$.15), but in poor agreement, outside the experimental limits, with the electron impact (0.33 $\pm$.07) and ion impact (0.29 $\pm$.07) values.

We conclude that the ion quasi-static theory gives the best description of the dependence of the observed broadening on principal quantum number, nuclear charge and plasma parameters.

6.2.2. Absolute Half-widths

Absolute half-widths for the ion quasi-static, electron impact and ion impact theories (equations 4,5 and 7 respectively) were calculated using the densities in Table 3. The electron impact broadening was calculated using values of T_e deduced from the free-bound continuum (see section 4.3), and the ion impact broadening was calculated using $\langle v \rangle = 3 \times 10^6 \text{cm s}^{-1}$ (see section 2.3). The half-widths calculated for the periods of separate and coincident emission varied by $\lesssim$ 20% from the average values which are shown in Table 4. This is in agreement with the fact that the experimental half-widths varied in time by $\lesssim$ 10% from their average values, which also are shown in Table 4. The errors indicated in Table 4 represent $\sim$ 80% confidence limits (the errors in the theoretical values include errors in the formulation of the equations, as well as in the plasma parameters). The theoretical ion half-widths are due predominantly to the ions C^{6+} and C^{5+}, rather than H^+.

TABLE 4

Theoretical and Experimental Full Half-widths

x (mm)	Line	$\Delta\lambda_{\frac{1}{2}}$ (Å) Theoretical			$\Delta\lambda_{\frac{1}{2}}$ (Å) Experimental
		ion quasi-static ± 50%	electron impact ± 55%	ion impact ± 60%	
1.0	C VI 5290	83	20	320	33 ± 3
	C VI 3434	30	4.5	73	12.8 ± 1.4
	C V 4945	75	14	280	38 ± 6
	C V 2982	23	2.8	50	10.6 ± 1.8
1.6	C VI 5290	41	6.6	110	21 ± 3
	C VI 3434	15	1.5	26	6.8 ± 1.0
	C V 4945	37	5.0	80	18 ± 5
	C V 2982	12	0.9	15	6.6 ± 1.4

A comparison of the theoretical values in Table 4 shows (i) that the ion half-widths are greater than the electron half-widths, which indicates that the ions are likely to be the dominant cause of braodening, and (ii) that the ion quasi-static half-widths are smaller than the ion impact half-widths, which indicates that the ion quasi-static theory is likely to be the more relevant theory - see the discussion in Griem and Shen, 1961, p.1494.

A comparison of the theoretical and experimental half-widths shows that the electron impact broadening, which is unlikely to be in error by more than a factor of two, amounts to $\sim$ 30% of the observed broadening. The majority of the observed broadening is therefore due to the ions.

The theoretical condition for the quasi-static theory to give a valid description of the broadening in the region of the half-width is that $\Delta\omega_{\frac{1}{2}} >> \langle v \rangle N_p^{1/3}$ (see, e.g. Griem, 1967 b). Substituting for $\Delta\omega_{\frac{1}{2}}$ from equation 4, this condition becomes $N(C^{6+}) >> 10^{14} cm^{-3}$, $N(H^+) >> 10^{16} cm^{-3}$ and $N_e >> 10^{23} cm^{-3}$. Inspection of the densities in Table 3 shows that the quasi-static theory is valid for the ions but not for the electrons.

The conclusion, based on the experimental and theoretical results, in this and the previous section, is that the broadening is predominantly ion quasi-static with C^{6+} and C^{5+} as the principal perturbing ions.

Finally, we note from Table 4 that the theoretical estimates of the ion quasi-static half-widths are a factor of two greater than the observed half-widths. The same result emerges from a comparison with the preliminary line profile calculations of Peach (see section 6.2). This difference may be partly experimental, due to errors in the spatial resolution (the density and line width both vary rapidly over quite short distances); but may also be partly theoretical, due to insufficient allowance being made for the specialised nature of the plasma (the ions are streaming, with significant ion-ion interaction and with a possibly non-thermal relative velocity distribution).

7. CONCLUSION

Observations have been made, with good time and space resolution, of the intensities and wavelength profiles of the spectral lines C VI (6-7) 3434, (7-8) 5290 Å and C V (5-6) 2982, (6-7) 4945 Å in the plasma produced when a ruby laser pulse of energy 5 J and duration 17 ns at half-maximum is focused onto a polyethylene foil in vacuum. Absolute line intensities were interpreted with the aid of space scans and independent measurements of electron temperature to give values of electron and ion densities (Table 3 and fig. 2). Wavelength profiles were studied from close to the target where the broadening is predominantly Stark, to a distance of 12 mm from the target where only the residual Doppler broadening due to the plasma streaming motion is observed.

Stark profiles are presented in figures 4-7 for the plasma conditions indicated in section 4.3. Stark theory of relevance to these new lines has been reviewed, and expressions have been proposed for half-widths (section 2). A comparison between theory and experiment, involving both relative and absolute half-widths shows that the broadening is predominantly ion quasi-static, with C^{6+} and C^{5+} as the principal perturbing ions. The electron impact broadening, though substantially reduced by correlations in the perturbations of the upper and lower states, still amounts to $\sim$ 30% of the observed broadening.

There is a factor of two difference between theoretical and experimental half-widths, and this is about the maximum which can be explained in terms of errors in the experiment and in the formulation of the Stark theory.

8. ACKNOWLEDGEMENTS

I would like to express my thanks for the encouragement I have received for this work from Dr R W P McWhirter (of the Astrophysics Research Unit) and from Dr N J Peacock. I am grateful to Professor H R Griem and to Dr G Peach for several very helpful discussions, and in particular to Professor H R Griem for the provision of equations 2, 5 and 6. I would also like to thank Mr J Payne for his assistance with the operation of the laser, and Dr N J Peacock for his criticism of the manuscript.

9. REFERENCES

AGLITZKY, E.V., BOIKO, V.A., ZAKHAROV, S.M. and SKLIZKOV, G.V., 1970, Lebedev Institute Report No. 143.

AGLITZKY, E.V., BASOV, N.G., BOIKO, V.A., GRIBKOV, V.A., ZAKHAROV, S.A., KROKHIN, O.N., and SKLIZKOV, G.V., 1971 Tenth International Conference on Phenomena in Ionised Gases, Oxford, p.229.

AMBARTSUMYAN, R.V., BASOV, N.G., BOIKO, V.A., ZUEV, V.S., KROKHIN, O.N., KRYUKOV, P.G., SENAT-SKII, Yu. V. and STOILOV, Yu. Yu., 1965, Zh. Eksp. Teor. Fiz., 48, 1583-7. (J.E.T.P. 21, 1061-4, 1965).

BACON, M.E., 1969, Ph.D. Thesis, Colorado State University.

BASHKIN, S., 1970, Nuclear Insts. and Methods, 90, 3-13.

BASOV, N.G., GRIBKOV, V.A., KROKHIN, O.N. and SKLIZKOV, G.V., 1968, Zh. Eksp. Teor. Fiz., 54, 1073-87 (J.E.T.P. 27, 575-82, 1968).

BATES, D.R., and DAMGAARD, A., 1949, Phil. Trans. R. Soc. 242 A, 101-22.

BOLAND, B.C. and IRONS, F.E., 1967, Seventh International Conference on Phenomena in Ionized Gases, Vienna, p.452.

BOLAND, B.C., IRONS, F.E. and McWHIRTER, R.W.P., 1968, J. Phys. B, 1, 1180-91.

BURGESS, D.D., FAWCETT, B.C. and PEACOCK, N.J., 1967, Proc. Phys. Soc. 92, 805-16.

COOPER, J., 1966, Reports on Progress in Physics, 29, 35-130.

DUPREE, A.K. and GOLDBERG, L., 1970, Ann. Rev. of Astron. and Astroph., 8, 231-264.

EDLÉN, B. and LÖFSTRAND, B., 1970, J. Phys. B., 3, 1380-88.

EVTUSHENKO, T.P., ZAIDEL', A.N., OSTROVSKAYA, G.V. and CHELIDZE, T. Ya., 1966, Zh. Tekh. Fiz., 36, 1506-13, (Sov. Phys. - Tech. Phys., 11, 1126-30, 1967).

FAUGERAS, P.E., MATTIOLI, M. and PAPOULAR, R., 1968, Plasma Phys., 10, 939-49.

GRIEM, H.R., 1960, Astroph., J. 132, 883-93.

GRIEM, H.R., 1967 a, Astroph. J., 147, 1092-9.

GRIEM, H.R., 1967 b, Astroph. J., 148, 547-58.

GRIEM, H.R. and SHEN, K.Y., 1961, Phys. Rev., 122, 1490-6.

GRIEM, H.R. and KUNZE, H.J., 1969, Phys. Rev. Letts., 23, 1279-81.

HALLIN, R. and HUGHES, T.P., 1961, Proc. Phys. Soc., 78, 201-3.

HOOPER, C.F. Jr., 1968, Phys. Rev. 165, 215-22.

IRONS, F.E., McWHIRTER, R.W.P. and PEACOCK, N.J., 1972, to be published in J. Phys. B.

LITVAK, M.M. and EDWARDS, D.F., 1966, J. Appl. Phys., 37, 4462-74.

MANDEL'SHTAM, S.L., PASHININ, P.P., PROKHINDEEV, A.M., PROKHOROV, A.M. and SUKHODREV, N.K., 1964, Zh. Eksp. Teor. Fiz., 47, 2003-5, (J.E.T.P. 20, 1344-6, 1965).

MARGENAU, H. and LEWIS, M., 1959, Rev. Mod. Phys. 31, 569-615.

MATTIOLI, M. and VÉRON, D., 1969, Plasma Phys. 11, 684-6.

MATTIOLI, M. and VÉRON, D., 1970, Phys. Fluids, 14, 717-21.

McWHIRTER, R.W.P. and HEARN, A.G., 1963, Proc. Phys. Soc. 82, 641-54.

PEACH, G., 1971, VIIth Int. Conf. on the Physics of Electronic and Atomic Collisions, Amsterdam, 1149-51.

RAMSDEN, S.A. and DAVIES, W.E.R., 1964, Phys. Rev. Letts., 13, 227-9.

WIESE, W.L., SMITH, M.W. and GLENNON, B.M., 1966, National Standard Reference Data Series, Report NSRDS - NBS4, Washington, 1, 1-152.

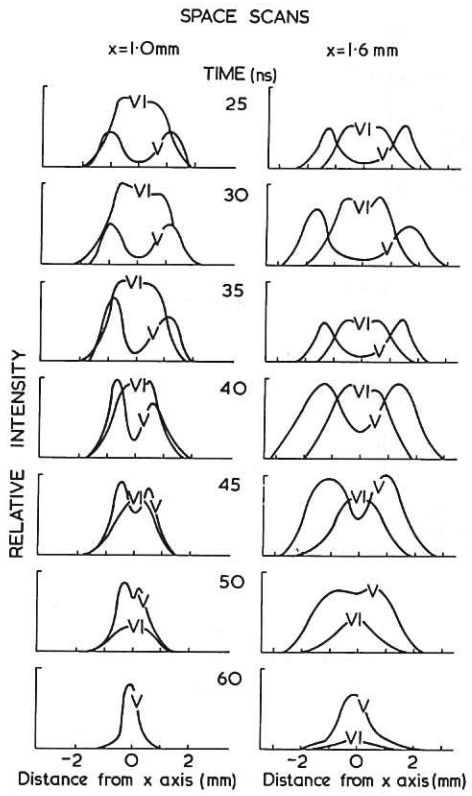

Fig.1 Space scans of C V and C VI radiation (indicated by 'V' and 'VI' respectively) as a function of time at x = 1.0 and 1.6 mm. The smooth curves represent the best fit to data points recorded by the technique of Irons et al (1972). The peak laser intensity corresponds to the time t = 20 ns.

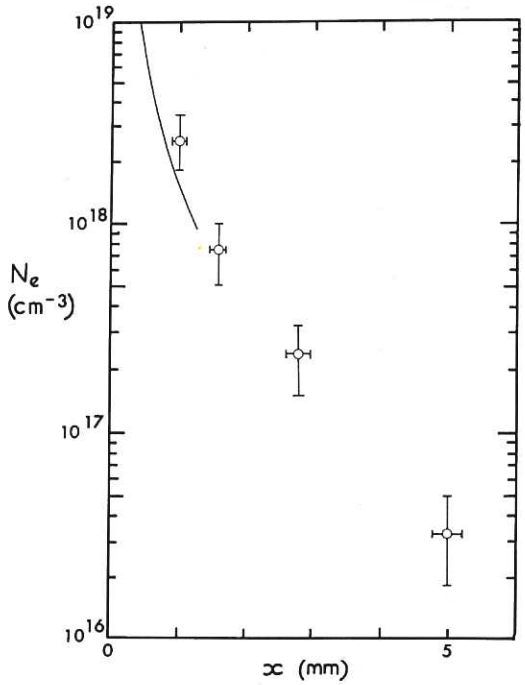

Fig.2 Electron density as deduced from the absolute intensities of spectral lines of C V and C VI (ϕ), and for comparison the electron density in a similar plasma (Aglitzky et al, 1970) as deduced from interferometry.

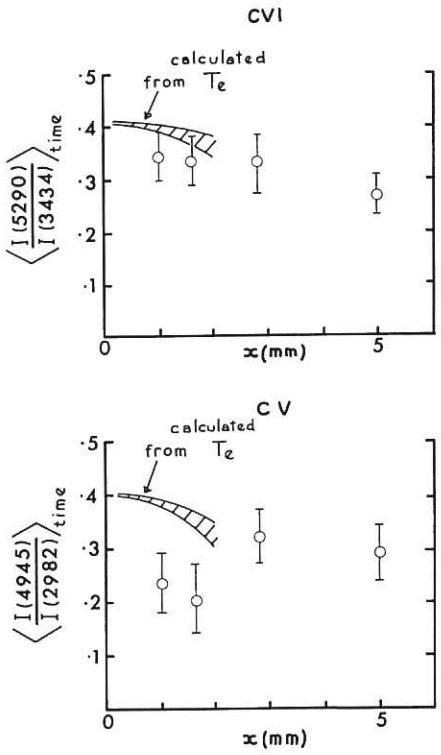

Fig.3 Experimental (ϕ) values of the intensity ratios $\frac{I(5290)}{I(3434)}$ for C VI and $\frac{I(4945)}{I(2982)}$ for C V at x = 1-5 mm. Also shown (as an area between two curves which represent the limits of uncertainty) are theoretical values of the same ratios calculated by means of equation 8 for values of T_e deduced independently from the free-bound continuum.

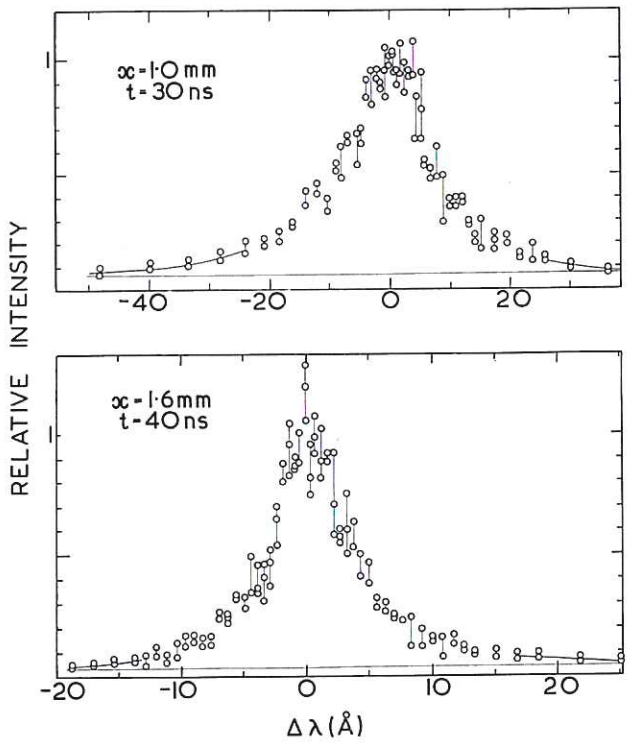

Fig.4 Typical Stark profiles of C VI 3434 Å at x = 1.0 and 1.6 mm. The data (o) for the two or three shots at each wavelength have been joined by vertical lines to show the shot-to-shot spread in intensity. The continuum level is shown.

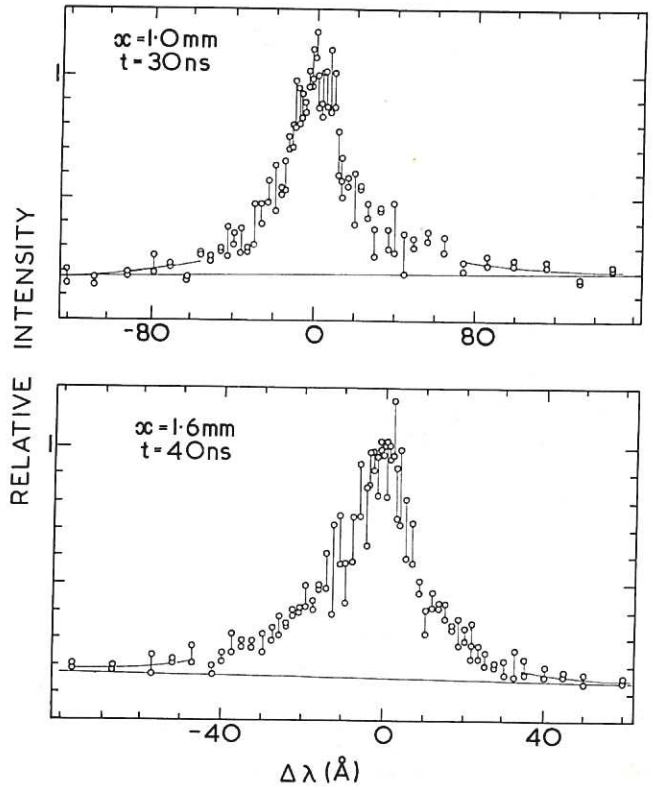

Fig.5 Typical Stark profiles of C VI 5290 Å at x = 1.0 and 1.6 mm. The data (o) for the two or three shots at each wavelength have been joined by vertical lines to show the shot-to-shot spread in intensity. The continuum level is shown.

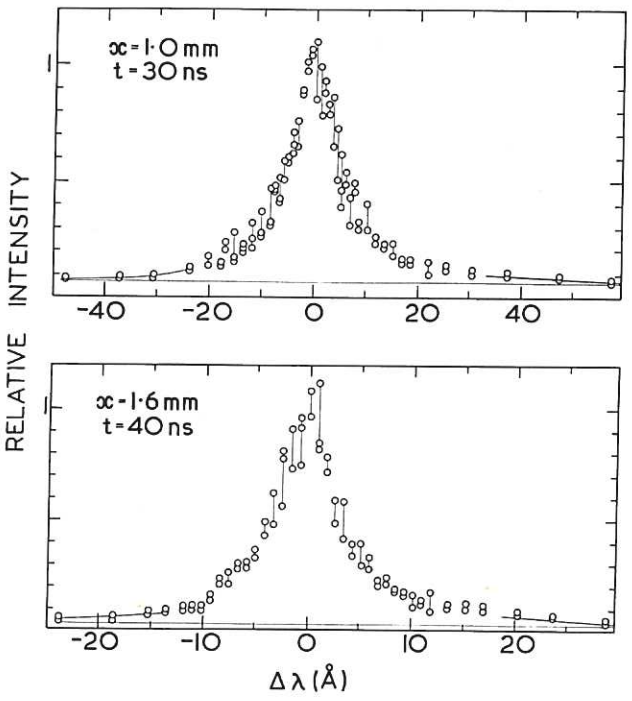

Fig.6 Typical Stark profiles of C V 2982 Å at x = 1.0 and 1.6 mm. The data (o) for the two or three shots at each wavelength have been joined by vertical lines to show the shot-to-shot spread in intensity. The continuum level is shown.

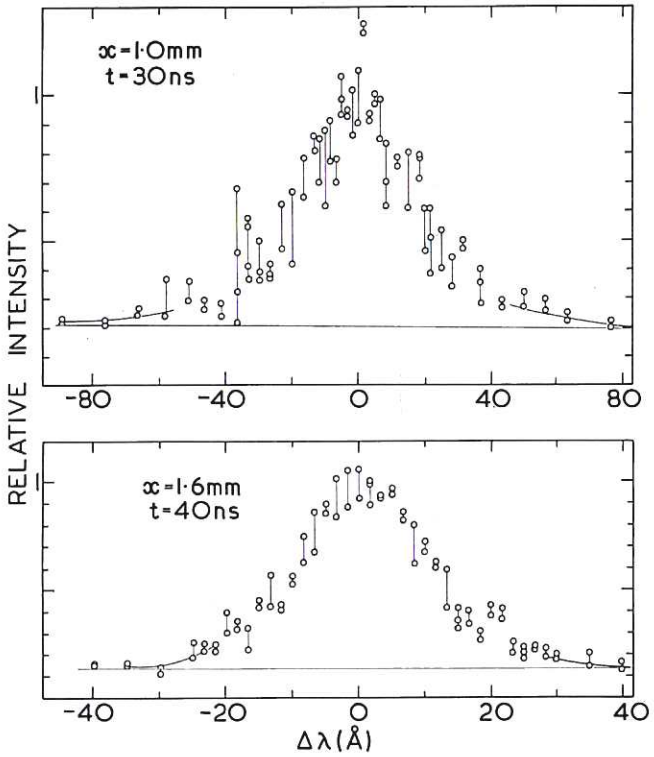

Fig.7 Typical Stark profiles of C V 4945 Å at x = 1.0 and 1.6 mm. The data (o) for the two or three shots at each wavelength have been joined by vertical lines to show the shot-to-shot spread in intensity. The continuum level is shown.

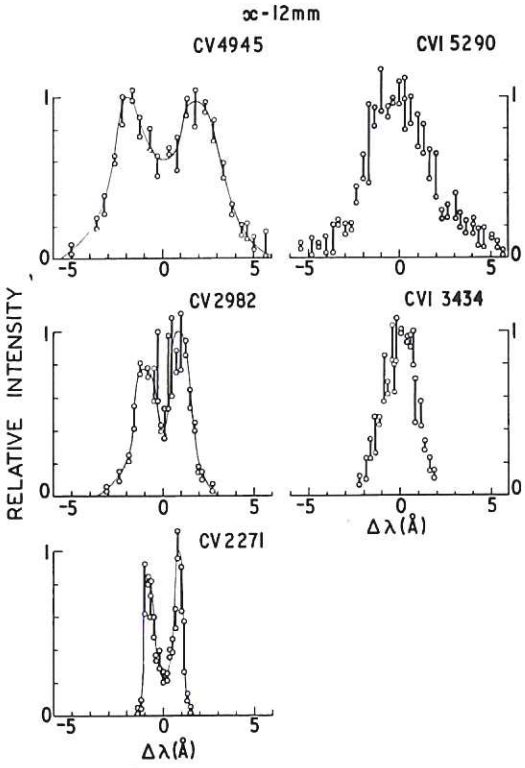

Fig.8 Doppler profiles of C VI 3434, 5290 and C V 2271, 2982 and 4945 Å at x = 12 mm, typical of the period of separate emission. The data (o) for the two or three shots at each wavelength have been joined by vertical lines to show the shot-to-shot spread in intensity. Smooth curves of visual best fit to the data points have been drawn.

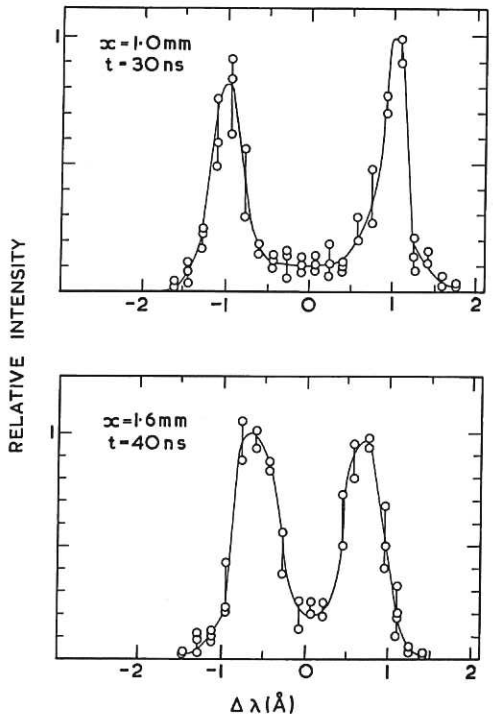

Fig.9 Doppler profiles of C V 2271 Å at x = 1.0 and 1.6 mm, typical of the period of separate emission. The data (o) for the two or three shots at each wavelength have been joined by vertical lines to show the shot-to-shot spread in intensity. Smooth curves of visual best fit to the data points have been drawn.

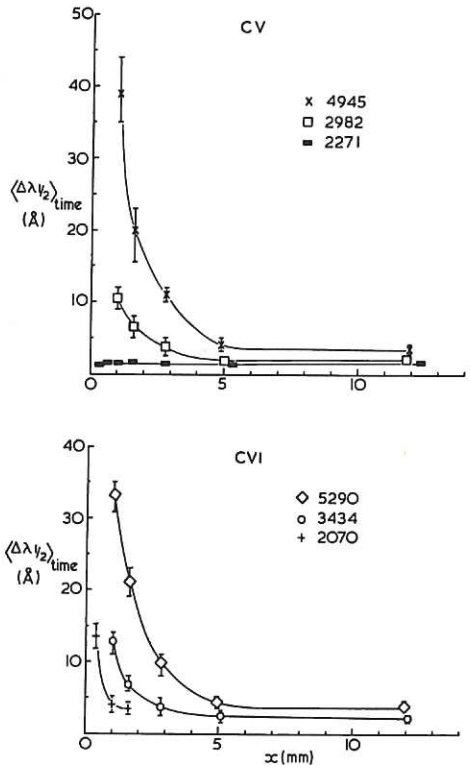

Fig.10 Time-average values of the full half-widths, $\Delta\lambda_{\frac{1}{2}}$, for the lines C V 2271, 2982, 4945 (top graph) and C VI 2070, 3434, 5290 (bottom graph), at x = 0.35 - 12 mm. The experimental points for each line have been joined by a smooth curve to show the trend.

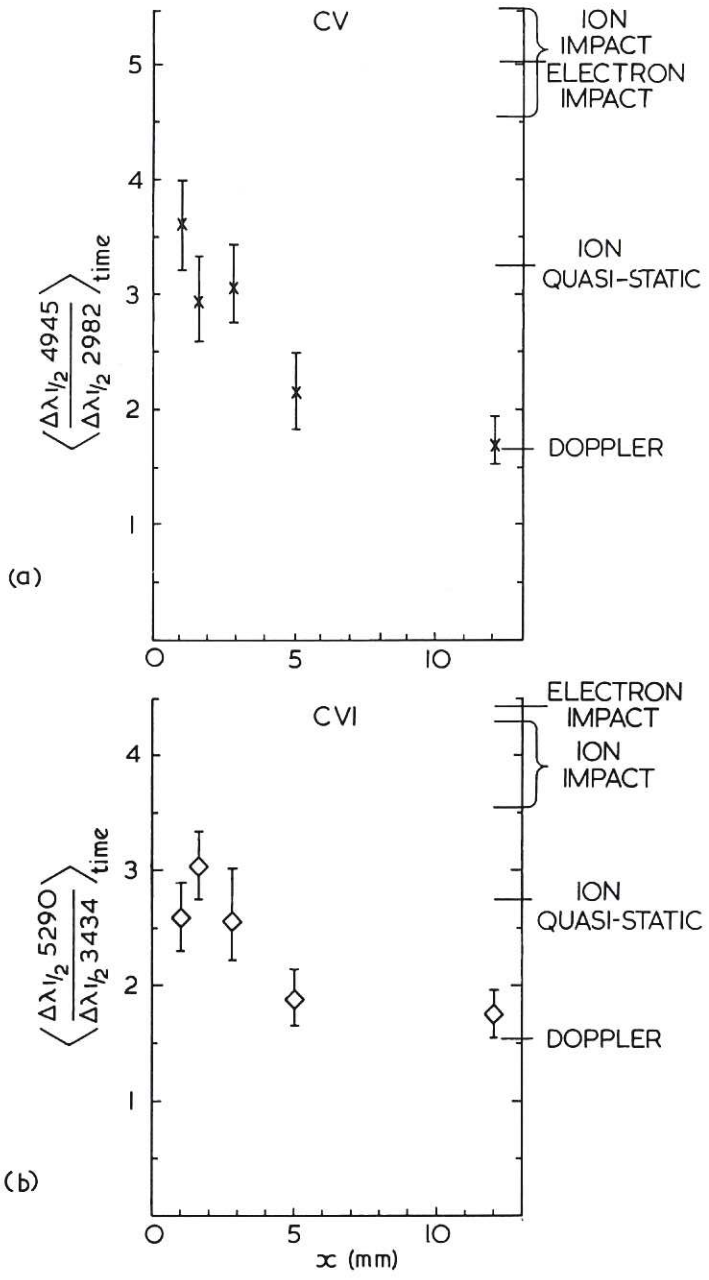

Fig.11 Time-average values of the half-width ratios $\frac{\Delta\lambda_{\frac{1}{2}}4945}{\Delta\lambda_{\frac{1}{2}}2982}$ for C V (top graph) and $\frac{\Delta\lambda_{\frac{1}{2}}5290}{\Delta\lambda_{\frac{1}{2}}3434}$ for C VI (bottom graph) at x = 1.0 - 12 mm. The values predicted by the ion quasi-static, electron impact, ion impact and Doppler theories of broadening are marked on the righthand ordinate.